T. Bierkandt, P. Hemberger, P. Oßwald, N. Gaiser, M. Hoener, D. Krüger, T. Kasper, M. Köhler, A combustion chemistry study of tetramethylethylene in a laminar premixed low-pressure hydrogen flame, Proc. Combust. Inst. 39 (2023) 1699-1708.

The original publication is available at www.elsevier.com

https://doi.org/10.1016/j.proci.2022.07.205

A combustion chemistry study of tetramethylethylene in a laminar premixed low-pressure hydrogen flame

Thomas Bierkandt[a,*], Patrick Hemberger[b], Patrick Oßwald[a], Nina Gaiser[a], Martin Hoener[c], Dominik Krüger[d], Tina Kasper[c,e], Markus Köhler[a]

[a]*Institute of Combustion Technology, German Aerospace Center (DLR), Pfaffenwaldring 38-40, 70569 Stuttgart, Germany*
[b]*Laboratory for Synchrotron Radiation and Femtochemistry, Paul Scherrer Institute, 5232 Villigen, Switzerland*
[c]*Mass Spectrometry in Reactive Flows, University of Duisburg-Essen, Lotharstraße 1, 47057 Duisburg, Germany*
[d]*Division 9, State Health Office, Nordbahnhofstraße 135, 70191 Stuttgart, Germany*
[e]*Technical Thermodynamics, Paderborn University, 33098 Paderborn, Germany*

Abstract

The combustion chemistry of tetramethylethylene (TME) was studied in a premixed laminar low-pressure hydrogen flame by combined photoionization molecular-beam mass spectrometry (PI-MBMS) and photoelectron photoion coincidence (PEPICO) spectroscopy at the Swiss Light Source (SLS) of the Paul Scherrer Institute in Villigen, Switzerland. This hexene isomer with the chemical formula C_6H_{12} has a special structure with only allylic C-H bonds. Several combustion intermediate species were identified by their photoionization and threshold photoelectron spectra, respectively. The experimental mole fraction profiles were compared to modeling results from a recently published kinetic reaction mechanism that includes a TME sub-mechanism to describe the TME/H_2 flame structure. The first stable intermediate species formed early in the flame front during the combustion of TME are 2-methyl-2-butene (C_5H_{10}) at a mass-to-charge ratio (*m/z*) of 70, 2,3-dimethylbutane (C_6H_{14}) at *m/z* 86, and 3-methyl-1,2-butadiene (C_5H_8) at *m/z* 68. Isobutene (C_4H_8) is also a dominant intermediate in the combustion of TME and results from consumption of 2-methyl-2-butene. In addition to these hydrocarbons, some oxygenated species are formed due to low-temperature combustion chemistry in the consumption pathway of TME under the investigated flame conditions.

Keywords: Tetramethylethylene; 2,3-Dimethyl-2-butene; Synchrotron vacuum ultraviolet (VUV) photoionization; Molecular-beam mass spectrometry (MBMS); Photoelectron photoion coincidence (PEPICO) spectroscopy

---

*Corresponding author.
E-mail address: thomas.bierkandt@dlr.de (T. Bierkandt)

1. Introduction

Tetramethylethylene (TME), also known as 2,3-dimethyl-2-butene, has the chemical formula C_6H_{12} and is the simplest tetra-substituted alkene. Its special structure opens the opportunity to study the combustion of a hydrocarbon that has only allylic C-H bonds. In total, tetramethylethylene has 12 allylic C-H bonds, in which the hydrogen atom is bound to a sp^3 carbon atom in vicinity to a C-C double bond. Any hydrogen abstraction results in the same resonance-stabilized C_6H_{11} radical and allylic C-H bonds are significantly weaker than primary (alkylic) or vinylic C-H bonds [1]. Despite its interesting structure, combustion of TME is not well-studied. Hydrogen abstraction of TME to form the 2,3-dimethyl-2-buten-1-yl radical (C_6H_{11}) was investigated by Krüger et al. [2] in previous work and compared to different C_2 (ethane) and C_4 (*n*-butane, isobutane, 1-butene, and isobutene) hydrocarbons under similar conditions utilizing doped hydrogen flames. They found a clear hydrogen abstraction order of tertiary > primary, secondary > primary, and allylic > non-resonance-stabilized for the investigated hydrocarbon fuels. McEnally and Pfefferle [3] studied the decomposition of tetramethylethylene and all other hexene isomers in methane/air laminar non-premixed flames by photoionization mass spectrometry. They showed that isomerization is a minor decomposition step of TME in contrast to all other hexenes and instead formation of 2,3-dimethyl-1,3-butadiene (C_6H_{10}) by scission of allylic C-H bonds is favored. For the hexene isomers, and for alkene fuels in general, it can be concluded that the more allylic CH bonds present, the less reactive the fuel is [4] and TME is the only hexene isomer which has only allylic and no vinylic C-H bonds. Wu et al. [5] used TME in a five components surrogate gasoline fuel to cover the alkene content of commercial gasoline. Baldwin et al. [6] investigated the addition of HO_2 radicals to ethylene (C_2H_4) and TME (C_6H_{12}) by formation of oxirane and tetramethyloxirane, respectively. They found that tetramethylethylene has a significantly lower activation energy for this addition reaction. Absolute rate constants for the addition of oxygen atoms to tetramethylethylene, which showed a strong negative temperature dependence, were investigated by Biehl et al. [7] in the temperature range of 200 to 370 K. Some authors [8-11] have also studied the ozonolysis of tetramethylethylene.

We report the investigation of the chemical structure of a TME-doped H_2 flame. Several combustion intermediates were identified by their photoionization or photoelectron spectra and quantified to present mole fraction profiles. Decomposition of tetramethylethylene is discussed based on the experimental results and the kinetic modeling results of the recently published high-temperature mechanism NUIGMech1.1_HT from NUI Galway [12-14]. For main intermediates in TME decomposition, additional modeling results from a modified version of NUIGMech1.1_HT and the new NUIGMech1.2 [15] with detailed high- and low-temperature chemistry are also considered.

2. Experiment

The total gas flow of the TME-doped hydrogen flame was 4067 sccm (1.65 mol-% TME, 44.26 mol-% H_2, 29.50 mol-% O_2, and 24.59 mol-% Ar). This fuel-rich flame with an equivalence ratio of 1.25 was stabilized at 40 mbar on a water-cooled McKenna-type burner with a porous sintered bronze matrix that has a diameter of 60 mm. Combustion gases were sampled by a quartz nozzle with an orifice diameter of about 300 µm directly from the flame. Due to the large pressure drop between the flame chamber and the first pumping stage, a molecular beam is formed. The central core of this molecular beam is skimmed and sampled molecules were analyzed by photoelectron photoion coincidence spectroscopy (PEPICO), i.e., ions and electrons are measured after the ionization event in coincidence [16]. The molecular-beam technique prevents a change of the gas composition during the sampling process and even allows for the detection of very elusive and reactive species such as radicals. Experiments were realized at the VUV beamline of the Swiss Light Source (SLS), where vacuum ultraviolet (VUV) synchrotron radiation enables the identification of isomers due to the high energy resolution and the tunability of the photon energy. A more detailed description of the flame experiment and the beamline was given by Oßwald et al. [17] and in a recently published review article by Hemberger et al. [18]. Photoionization (PI) and threshold photoelectron (TPE) spectra were obtained by scanning the photon energy at a constant burner position of 1.75 mm in the reaction zone of the flame. Isomer-resolved mole fraction profiles were measured by sampling the gas composition at heights above the burner (HAB) between 0.25 and 30.25 mm for several photon energies.

3. Results and discussion

A study by Krüger et al. [2] investigated the hydrogen abstraction from TME to produce the fuel radical C_6H_{11} (2,3-dimethyl-2-buten-1-yl radical) in the same flame and compared it to the first hydrogen abstraction reaction in other alkane- and alkene-doped H_2 flames. In our study, more than 30 combustion species were identified in the TME-doped H_2 flame, and their mole fraction profiles determined. All mole fraction profiles and the temperature profile are available for download as supplementary material. General uncertainty of the mole fractions is 15-20% for main species, 30-50% for combustion intermediates with known photoionization cross section (PICS), and a factor of 2-4 for species with unknown, i.e., estimated, PICS [19, 20]. The uncertainty of the flame temperature determination

using thermocouples is comparable to optical methods and is estimated to be 5-10% [20].

Figure 1 shows the measured mole fraction profiles of the main species, i.e., the fuels TME and H_2, the oxidizer O_2, the diluent gas Ar, and the combustion products H_2O, CO, and H_2O, in comparison to the modeling results. Unless otherwise noted, the high-temperature version of the NUIGMech1.1 (NUIGMech1.1_HT with release date October 2nd, 2020) [12-14] was used for simulations, which were done with the software library Cantera [21] and with the Cantera flame reactor module for burner-stabilized flames within the Chemical Workbench [22]. The exhaust gas concentrations and mole fractions in the reaction zone of the flame are within the uncertainty of the experiment. However, there are larger deviations in the preheating zone, where the observed consumption of the fuels and the oxidizer is more pronounced than predicted by the model. Hence, higher concentrations of H_2O, CO, and CO_2 are already detected.

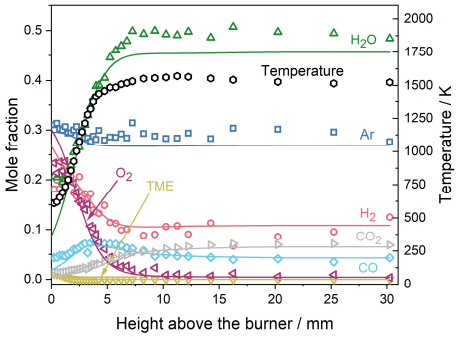

Fig. 1. Mole fraction profiles of the main combustion species and the diluent gas (symbols: experiment; solid lines: simulation) as well as the temperature profile (dashed line).

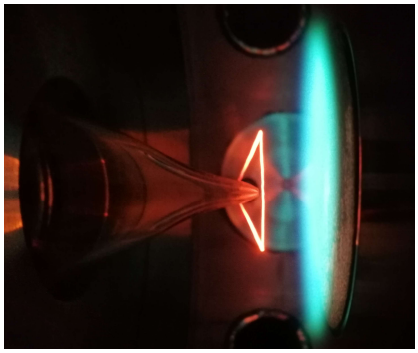

Fig. 2. Flame temperature measurement by a thermocouple in presence of the sampling nozzle.

The temperature profile that was used as input for the kinetic modeling is also presented in Fig. 1. The profile was determined from the temperature dependence of the sampling rate through the quartz nozzle [23] by using the exhaust gas temperature of a propane-doped hydrogen flame with an identical C:H:O ratio to the TME/H_2 flame. It was shown by Krüger et al. [2] that the hydrocarbon-doped hydrogen flames have identical temperature profiles under the investigated conditions so that it is appropriate to use the measured exhaust temperature from the propane/H_2 flame. The used thermocouple had a small bead diameter of 130 µm and was coated by non-catalytic SiO_2. It was positioned very close to a quartz sampling nozzle as shown in Fig. 2 to consider the influence of the nozzle on the flame temperature. The radiation correction was done according to Gonchikzhapov and Kasper [24] and the entire procedure for obtaining the temperature profile is described in detail in the supplementary material.

Sensitivity of the simulation results on the temperature profile was evaluated by using profiles with increased (+10%) and decreased (-10%) temperature. Results for main species and selected intermediates that are discussed below are presented in Fig. S1 and S2, respectively. Exhaust gas concentrations of H_2, H_2O, CO, and CO_2 are still within the uncertainty range of ±20% for main species. For mole fraction profiles of intermediate species, changes in absolute concentrations are minor and mainly spatial shifts are observed. Overall, the peak positions of many intermediate species are well predicted by simulations with the original temperature profile from Fig. 1, which also best predicts the consumption of TME and O_2 in the reaction zone.

Figure 3 shows the mole fraction profiles of typical C_1-C_3 combustion intermediates (CH_3, C_2H_2, C_2H_4, CH_2O, C_3H_4, and C_3H_6) often formed during combustion of hydrocarbons and some specific species (C_4H_8, C_5H_8, and C_5H_{10}) directly related to the fuel structure. Literature photoionization cross sections exist for all species presented in Fig. 3, and the resulting maximum experimental uncertainty of 50% is indicated. Considering the experimental uncertainty and the general uncertainty of the modeling, most species are satisfactorily reproduced and the used high-temperature mechanism NUIGMech1.1_HT appears suitable to predict the decomposition of TME under the investigated conditions. Contrasting the results for the aforementioned species, formation of isobutene (C_4H_8) is substantially underestimated by this model and that of propene (C_3H_6) and 2-methyl-2-butene (C_5H_{10}) are overestimated. Reactions with H atoms are key reactions in alkene oxidation [4] and particularly important in the hydrogen-rich environment studied here. Updating the rate constants for reactions of H atoms with C_2-C_4 alkenes (ethylene, propene, isobutene, 1-butene, and 2-butene) and pentene isomers (2-methyl-1-butene, 2-methyl-2-butene, and 3-methyl-1-butene) from the theoretical work of Power et al. [25, 26] substantially improve the prediction of the isobutene mole fraction as shown in Fig. 3, where the modified mechanism is denoted as NUIGMech1.1_HT_mod. Predictions of ethylene and propene are also improved, while the mole fraction of 2-methyl-2-butene is even more overestimated.

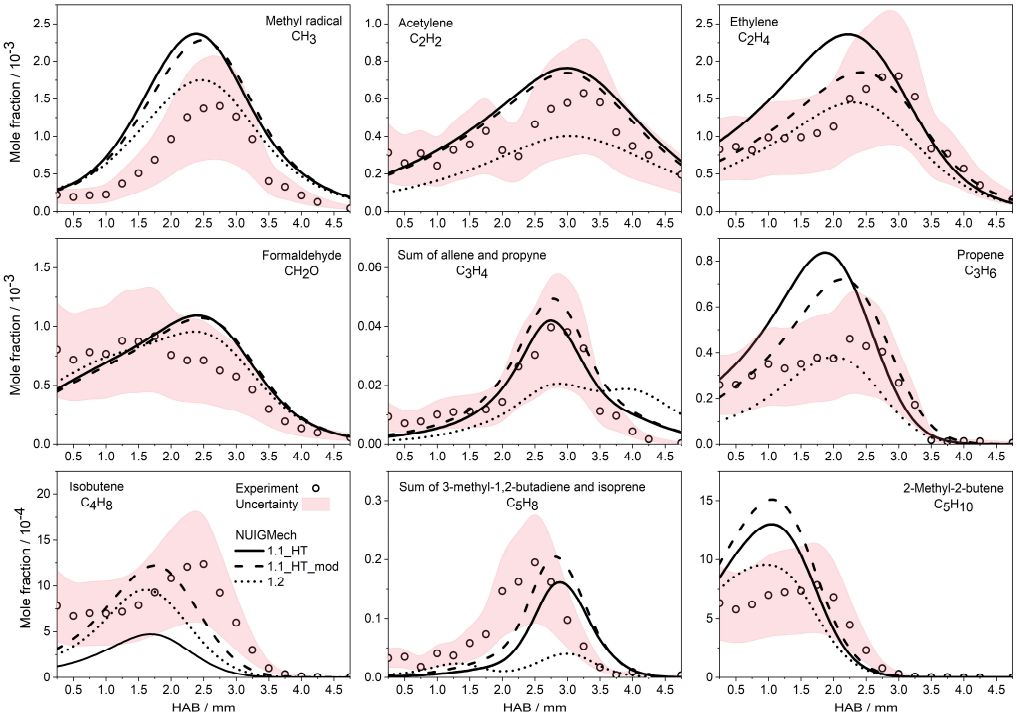

Fig. 3. Mole fraction profiles of some C_1-C_5 combustion intermediates measured in the TME/H_2 flame and comparison to the simulation results. Symbols: experimental data; shaded area: experimental uncertainty of 50%; solid lines: modeling results.

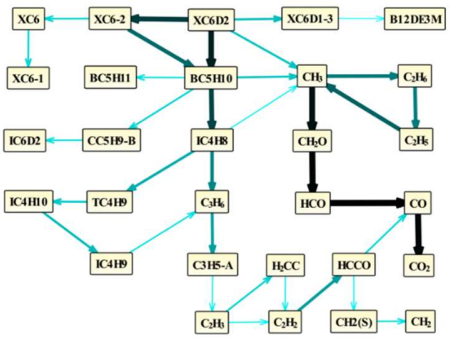

Fig. 4. Rate of production (ROP) analysis of the total carbon flux in the entire TME/H_2 flame. Only carbon fluxes higher than 8% are shown.

For most intermediates, improved agreement with the experimental mole fraction profiles can be achieved with the latest NUI Galway mechanism (NUIGMech1.2) by Sahu et al. [15]. This mechanism has also implemented the previously mentioned updates by Power et al., but also includes detailed low-temperature chemistry. As seen in Fig. 3, the three main intermediates 2-methyl-2-butene (C_5H_{10}), isobutene (C_4H_8), and propene (C_3H_6), whose formation is directly linked to the fuel decomposition over the reaction channel TME → 2-methyl-2-butene → isobutene → propene as discussed below, are now well predicted. On the other hand, predictions for the isomers C_3H_4 and C_5H_8 that have lower concentrations on the order of 10^{-5} deteriorate. Given that NUIGMech1.2 was used without modifications and was not previously validated for TME, the overall agreement between experimental mole fraction profiles and modeling results is very good.

To further investigate the fuel decay, a rate of production (ROP) analysis was done for the entire flame and is presented in Fig. 4, where the thickness of the arrows represents the carbon flux between species. Three main consumption pathways of TME (XC6D2) can be identified: (R1) Hydrogen atom addition reaction to yield the C_6H_{13} radical 2,3-dimethylbut-2-yl (XC6-2)

$$XC6D2 + H = XC6\text{-}2 \quad (R1)$$

with a decay rate contribution of 34.9%, (R2) hydrogen atom induced substitution to yield 2-methyl-2-butene (BC5H10) and the methyl radical

$$XC6D2 + H = BC5H10 + CH_3 \quad (R2)$$

with a contribution of 55.3%, and (R3) hydrogen atom abstraction reaction to yield the resonance-stabilized C_6H_{11} radical 2,3-dimethyl-2-buten-1-yl (XC6D1-3)

$$XC6D2 + H = XC6D1\text{-}3 + H_2 \quad (R3)$$

with a contribution of 9.6% to TME decay. Its resonance structure is the 2,3-dimethyl-1-buten-3-yl radical. The 2,3-dimethylbut-2-yl radical (XC6-2) also contributes significantly to the formation of 2-methyl-2-butene (BC5H10) by β-C-C-scission

$$XC6\text{-}2 = BC5H10 + CH_3 \qquad (R4)$$

making this species an important intermediate in the combustion of TME with a maximum mole fraction of about $1 \cdot 10^{-3}$ in both the experiment and simulations. Mole fraction profiles of the two fuel radicals formed by H abstraction (C_6H_{11}) and H addition (C_6H_{13}) reactions are presented in Fig. S3 in the supplementary material. Quantification is based on estimated cross sections and absolute values are therefore affected with high uncertainties, but the modeling results show that the predicted concentration of C_6H_{13} by NUIGMech1.2 is one order of magnitude smaller than the predictions of the high-temperature mechanisms and in better accordance to the experiment.

Figure 5 presents the measured photoelectron spectra at a mass-to-charge ratio (*m/z*) of 70 in the TME-doped hydrogen flame. 2-Methyl-2-butene at *m/z* 70 is unambiguously identified by its threshold photoelectron spectrum (TPES). The spectrum shows the vibrational fine structure of the first band corresponding to the C=C stretching mode with a vertical ionization energy of 8.86 eV [27] at the highest intensity transition and is well reproduced by two reference photoelectron spectra from the work of Pieper et al. [28] and Mintz and Kuppermann [27]. According to the rate of production analysis in Fig. 4, direct formation of isobutene (IC4H8) from 2-methyl-2-butene (BC5H10) by substitution reaction

$$BC5H10 + H = IC4H8 + CH_3 \qquad (R5)$$

is a main pathway in the TME/H_2 flame. Isobutene formation by β-CC-scission of the tertiary 2-methylbut-2-yl radical (BC5H11), which is itself formed by H atom addition to 2-methyl-2-butene, may also be likely, but is less pronounced in the used mechanism. Ruwe et al. [29] detected isobutene and 2-butene in a rich 2-methyl-2-butene laminar premixed low-pressure flame by photoionization mass spectrometry in comparably high concentrations and concluded that their formation occurs via the C_5H_{11} radicals formed by H addition from the fuel. In the TME/H_2 flame, we have only observed the formation of isobutene as verified by the photoelectron spectrum of *m/z* 56 from this flame in comparison to the spectrum of the neat substance (see Fig. 6). A TPE spectrum of *trans*-2-butene from direct calibration is also presented in Fig. 6 and further confirms the absence of 2-butene in the TME/H_2 flame. The TPE spectrum of 2-butene looks similar in shape, but is shifted to a ca. 100 meV lower photon energy. Depending on the model, the maximum mole fraction of isobutene is 6.2-10.6 times higher than that of 2-butene and generally corroborates a dominance of isobutene.

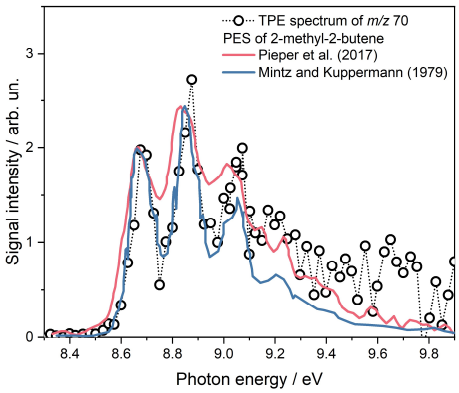

Fig. 5. Assignment of 2-methyl-2-butene to *m/z* 70 by photoelectron spectroscopy in the TME/H_2 flame.

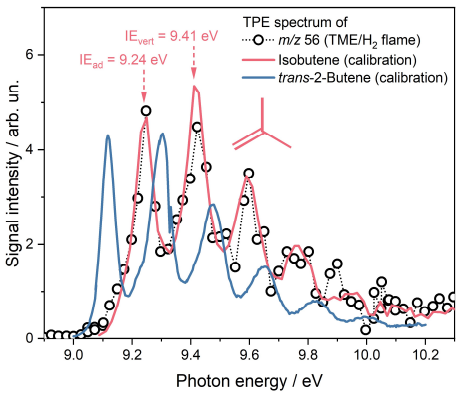

Fig. 6. Assignment of isobutene to *m/z* 56 by photoelectron spectroscopy in the TME/H_2 flame.

A second decomposition product of the C_6H_{13} radical (XC6-2) is 2,3-dimethylbutane (XC6) formed by a further hydrogen atom addition

$$XC6\text{-}2 + H = XC6 \qquad (R6)$$

as shown in the reaction path analysis in Fig. 4. At *m/z* 86, the hydrocarbon 2,3-dimethylbutane (C_6H_{14}), which has an ionization energy of 10.02 eV [30], cannot be identified with confidence from the PI or TPE spectrum. No increase in photoion yield is observed at the ionization energy of this species. Instead, the photoionization curve stagnates at about 10.5 eV (see Fig. 7) which is in accordance with the reference spectrum of 2,3-dimethylbutane measured by Wang et al. [31]. An onset in the PI spectrum is measured at a significantly lower photon energy of about 8.1 eV and a second increase of the signal between 9.25 and 9.3 eV is observed. Ionization energies of other C_6H_{14} isomers are in the range of 10.06 and 10.18 eV [30] so that their presence can be excluded and oxygenated species must be considered

instead. One possibility is the ketone 3-methyl-2-butanone ($C_5H_{10}O$) with an ionization energy of 9.31 eV [32]. It is predicted by the high-temperature models with a maximum mole fraction of about $4.1 \cdot 10^{-5}$ and in higher concentration of $1.7 \cdot 10^{-4}$ by the NUIGMech1.2. It is formed by unimolecular decomposition of the 1,1,2-trimethylpropoxy radical ($C_6H_{13}O$). The latter radical is formed in the mechanism via reaction of the C_6H_{13} radical 2,3-dimethylbut-2-yl (indicated as XC6-2 in the ROP analysis) with HO_2 and CH_3O_2 radicals, respectively. Our calculation of the adiabatic ionization energy for 3-methyl-2-butanone at the G4 level of theory [33] with Gaussian 16 [34] gives a value of 9.29 eV close to the literature value of 9.31 eV from [32]. A Franck-Condon simulation (FCS) was performed at the B3LYP\6-311G(2d,d,p) optimized geometries. This spectrum is also presented in Fig. 7 and confirms the presence of 3-methyl-2-butanone in the investigated flame. Franck-Condon simulations were also performed for 3,3-dimethyl-2-butanone (Fig. 8) and 2,3-dimethyl-1,3-butadiene (Fig. 9) at the same level of theory.

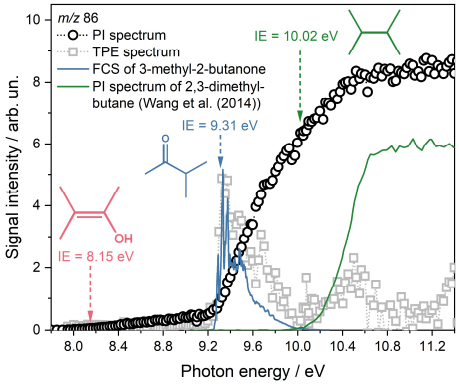

Fig. 7. Photoionization and threshold photoelectron spectra of *m/z* 86 measured in the TME/H_2 flame and comparison with a Franck-Condon simulation of 3-methyl-2-butanone and a literature spectrum of 2,3-dimethylbutane.

A possible oxygenate that may explain the onset at about 8.1 eV is the enol 3-methyl-2-buten-2-ol (C_5H_9OH) with an ionization energy of 8.15 eV [35]. It is not included in the mechanism, but could be directly formed from 2-methyl-2-butene (BC5H10) by a substitution reaction:

$$\text{BC5H10} + \text{OH} = C_5H_9OH + \text{H} \qquad \text{(R7)}$$

It has to be noted that several more $C_5H_{10}O$ isomers exist, but the presence of both the enol 3-methyl-2-buten-2-ol and its keto tautomer 3-methyl-2-butanone is plausible in the investigated TME/H_2 flame. Formation of these oxygenates may be enhanced by low-temperature oxidation chemistry, which has already been observed in other hydrocarbon-doped hydrogen flames with the identical C:H:O ratio [36] and can be more pronounced due to probe perturbations [37]. Probe perturbations have been extensively studied [19, 20, 38, 39] and the cooling effect of the sampling nozzle is sufficiently approximated for our 1D simulations using the perturbed temperature profile. However, there are other probe-induced effects that may affect the flame structure and can only be covered by 2D simulations. In particular, the distortion of the streamlines by the suction effect of the probe can explain deviations very close to the burner, but can be reduced by small orifice diameters [39].

Concentrations of many oxygenates are already near their maximum for the first 1.25 mm in the flame, where the measured temperature is below 740 K and falls into the low-temperature regime. They are better predicted by the NUIGMech1.2 as shown in Fig. S4 for ketene (C_2H_2O), acetaldehyde (CH_3CHO), acetone (C_3H_6O), and 3-methyl-2-butanone ($C_5H_{10}O$). Figure S5 shows two mass spectra recorded at a HAB of 1 mm for photon energies of 10.6 and 9.6 eV. This position corresponds to a flame temperature of about 690 K. The presence of methyl hydroperoxide (CH_3OOH) in the TME/H_2 flame can be clearly demonstrated by the measured photoionization spectrum at *m/z* 48 in comparison to a reference spectrum of the methyl hydroperoxide measured by Moshammer et al. [40] as shown in Fig. S6 in the supplementary material, which hints at the participation of the low-temperature oxidation chemistry in this flame. Formation of alkyl hydroperoxides was also observed in other alkane- and alkene-doped hydrogen flames in [36]. Other larger oxygenated species could be detected in the TME/H_2 flame, e.g., butanone at *m/z* 72 is clearly identified by comparison of the measured TPE spectrum with the reference spectrum of the neat substance by Kercher et al. [41] as presented in Fig. S7 in the supplementary material. The calculated maximum mole fraction of this oxygenated species, based on the PICS of butanal [42], is $3.1 \cdot 10^{-4}$ and all used mechanisms strongly underestimate the concentration.

A species with a significant higher mass than the hydrocarbon fuel TME was observed at *m/z* 100 as presented in Fig. 8 (see also the mass spectrum in Fig. S5). The onset of the PI spectrum is found at 8.6 eV. The signal slope increases at 9.1 eV, which may be caused by the oxygenate 3,3-dimethyl-2-butanone (also known as pinacolone), as suggested by the comparison of the measured photoelectron spectrum with a Franck-Condon simulation. The adiabatic ionization energy of 9.14 eV from the literature [32] closely matches our calculated value of 9.09 eV. A possible formation pathway can be found in the low-temperature chemistry according to Fish and Wilson [43], i.e., the oxidation of the 2,3-dimethylbut-2-yl radical by molecular oxygen to yield the 2-hydroperoxy-2,3-dimethylbut-3-yl radical ($C_6H_{13}O_2$), which then decomposes to 3,3-dimethyl-2-butanone ($C_6H_{12}O$) and OH according to R8:

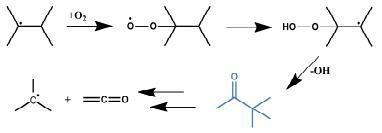

(R8)

Consumption of 3,3-dimethyl-2-butanone by H abstraction, followed by β-CC-scission would then yield ketene (C_2H_2O) and *tert*-butyl radicals (C_4H_9). *tert*-Butyl radicals have the lowest ionization energy of all butyl radicals and were clearly identified in the TME/H_2 flame by the onset at about 6.9 eV in the PI spectrum (see Fig. S8 in the supplementary material). They are also formed by hydrogen addition reaction from isobutene as presented in the ROP analysis (see Fig. 4) and their presence in the flame cannot be taken as confirmation for the formation of 3,3-dimethyl-2-butanone. In principle, the formation of O-heterocycles by decomposition of hydroperoxyalkyl radicals ($C_6H_{13}O_2$) and ring closure, e.g., 2,2,3-trimethyloxetane or 2,2,3,3-tetramethyloxirane, is also possible under low-temperature conditions as observed in the oxidation of 2,3-dimethylbutane [31, 43]. Experimental ionization energies of branched heptanes (C_7H_{16}) are unknown, their formation, however, is less likely, e.g., 2,2,3-trimethylbutane may be formed by recombination of the 2,3-dimethylbut-2-yl radical with methyl radicals. However, neither 3,3-dimethyl-2-butanone nor 2,2,3-trimethylbutane are included in the reaction mechanism.

The fuel radical, i.e., the C_6H_{11} radical (XC6D1-3 in the ROP analysis) decomposes to 3-methyl-1,2-butadiene (B12DE3M) and methyl radicals:

$$XC6D1\text{-}3 = B12DE3M + CH_3 \qquad (R9)$$

In Fig. S9 (see supplementary material), the measured photoionization spectrum at *m/z* 68 is well reproduced by both reference spectra of the C_5H_8 isomers 3-methyl-1,2-butadiene [42] and isoprene [44] up to a photon energy of 9.5 eV. Although the spectrum of the former species better represents the measured PI curve at higher photon energies, the presence of isoprene cannot be excluded. Hydrogen atom assisted isomerization of 3-methyl-1,2-butadiene to isoprene is also included in the reaction mechanisms. Therefore, the presented mole fraction of C_5H_8 in Fig. 3 is the sum of both discussed isomers and was calculated with the known photoionization cross section of 3-methyl-1,2-butadiene by Yang et al. [42]. Note that a higher mole fraction of isoprene is predicted by the model than for its isomer 3-methyl-1,2-butadiene. Instead of formation of 3-methyl-1,2-butadiene (C_5H_8) by β-CC-scission from the fuel radical (C_6H_{11}), 2,3-dimethyl-1,3-butadiene (C_6H_{10}) can also be formed by β-CH-scission. Its presence can be confirmed by the onset in the PI spectrum of *m/z* 82 at about 8.6 eV (see Fig. 9) that fits to the ionization energy of 8.62 eV for 2,3-dimethyl-1,3-butadiene measured by Bieri at al. [45] and the Franck-Condon simulation also fits to the measured TPE spectrum. The measured PI spectrum of the C_6H_{11} radical is presented in Fig. S10.

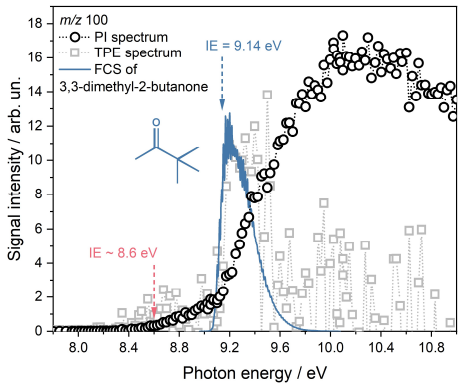

Fig. 8. Photoionization and threshold photoelectron spectra of *m/z* 100 measured in the TME/H_2 flame and comparison with a Franck-Condon simulation of 3,3-dimethyl-2-butanone.

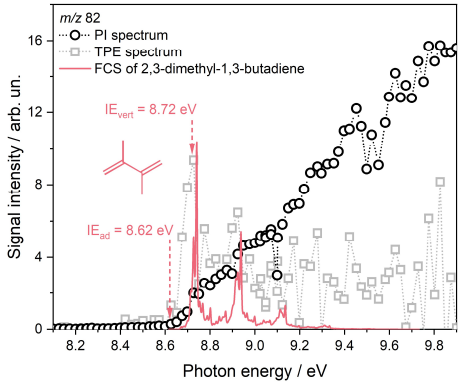

Fig. 9. Photoionization and threshold photoelectron spectra of *m/z* 82 measured in the TME/H_2 flame and comparison with a Franck-Condon simulation of 2,3-dimethyl-1,3-butadiene.

4. Conclusions

A laminar premixed low-pressure hydrogen flame doped with tetramethylethylene (TME) was investigated by photoionization mass spectrometry and photoelectron photoion coincidence spectroscopy. TME was chosen due to its special structure (i.e., it only contains allylic C-H bonds) and its decay is described based on the experimental and modeling results. Overall, three fuel consumption pathways can be identified. At *m/z* 70, 2-methyl-2-butene (C_5H_{10}) with an ionization energy of 8.69 eV is clearly identified by its photoelectron spectrum and is found in significant concentration in the flame. The formation of this species is directly linked to fuel decay by hydrogen addition to initially form the 2,3-dimethylbut-2-yl radical (C_6H_{13}) and by subsequent β-CC-scission of this radical. The reaction mechanism

also shows that this decomposition step is the most important one regarding the total carbon flux in the reaction path analysis and 2-methyl-2-butene is also formed directly from the fuel by a substitution reaction. The formation of 2-methyl-2-butene can explain the observation of isobutene in the investigated flame since it is a decomposition product of 2-methyl-2-butene. As expected, hydrogen abstraction by H and OH at one of the equivalent C-H bonds is also possible and results in the formation of the resonance-stabilized 2,3-dimethyl-2-buten-1-yl radical (C_6H_{11}) at *m/z* 83. This radical can decompose to 3-methyl-1,2-butadiene (C_5H_8) by β-CC-scission and 2,3-dimethyl-1,3-butadiene (C_6H_{10}) by β-CH-scission, respectively. Both species are identified in the investigated flame. The presence of isoprene (2-methyl-1,3-butadiene) at *m/z* 70 cannot be excluded since its ionization energy is very close to the ionization energy of 3-methyl-1,2-butadiene and rapid isomerization to isoprene by 1,2-H-shift reaction is known. The experimental results confirm the formation of a species with higher mass than the fuel at *m/z* 100. The photoionization spectrum at this mass-to-charge ratio has a distinct increase at about 9.1 eV, which agrees with 3,3-dimethyl-2-butanone ($C_6H_{12}O$). A plausible formation route proceeds via the 2-hydroperoxy-2,3-dimethylbut-3-yl radical due to low-temperature oxidation chemistry in the flame.

Acknowledgments

The authors gratefully acknowledge Luka Debenjak and Patrick Ascher for technical assistance, Andras Bodi for experimental research support, Munko Gonchikzhapov for assistance during temperature measurements, and all other members of the SLS flame team. The authors thank the German Research Foundation (DFG) for financial support under contract KA3871/3-2 and KO4786/2-2. Patrick Hemberger additionally thanks the Swiss Federal Office of Energy for financial support under contract SI/501269-01. The experiments were performed at the Swiss Light Source of the Paul Scherrer Institute in Villigen, Switzerland.

Supplementary material

Experimental mole fraction profiles, the temperature profile, and additional supporting figures are included in the supplementary material.

References

[1] D.F. McMillen, D.M. Golden, Hydrocarbon bond dissociation energies, *Ann. Rev. Phys. Chem.* 33 (1982) 493-532.

[2] D. Krüger, P. Oßwald, M. Köhler, P. Hemberger, T. Bierkandt, Y. Karakaya, T. Kasper, Hydrogen abstraction ratios: A systematic iPEPICO spectroscopic investigation in laminar flames, *Combust. Flame* 191 (2018) 343-352.

[3] C.S. McEnally, L.D. Pfefferle, Decomposition and hydrocarbon growth processes for hexenes in nonpremixed flames, *Combust. Flame* 143 (2005) 246-263.

[4] C.-W. Zhou, A. Farooq, L. Yang, A.M. Mebel, Combustion chemistry of alkenes and alkadienes, *Prog. Energy Combust. Sci.* 90 (2022) 100983.

[5] Y. Wu, B. Rossow, V. Modica, X. Yu, L. Wu, F. Grisch, Laminar flame speed of lignocellulosic biomass-derived oxygenates and blends of gasoline/oxygenates, *Fuel* 202 (2017) 572-582.

[6] R.R. Baldwin, D.R. Stout, R.W. Walker, Relative rate study of the addition of HO_2 radicals to ethylene and to tetramethylethylene, *J. Chem. Soc. Faraday Trans.* 80 (1984) 3481-3489.

[7] H. Biehl, J. Bittner, B. Bohn, R. Geers-Müller, F. Stuhl, Temperature dependence of the rate constants of the reactions of oxygen atoms with trans-2-butene, cis-2-butene, 2-methylpropene, 2-methyl-2-butene, and 2,3-dimethyl-2-butene, *Int. J. Chem. Kinet.* 27 (1995) 277-285.

[8] R.W. Murray, W. Kong, S.N. Rajadhyaksha, The ozonolysis of tetramethylethylene. Concentration and temperature effects, *J. Org. Chem.* 58 (1993) 315-321.

[9] M. Barton, J.R. Ebdon, A.B. Foster, S. Rimmer, Ozonolysis of tetramethylethylene: Characterization of cyclic and open-chain oligoperoxidic products, *J. Org. Chem.* 69 (2004) 6967-6973.

[10] X. Yang, J. Deng, D. Li, J. Chen, Y. Xu, K. Zhang, X. Shang, Q. Cao, Transient species in the ozonolysis of tetramethylethene, *J. Environ. Sci.* 95 (2020) 210-216.

[11] G.T. Drozd, J. Kroll, N.M. Donahue, 2,3-Dimethyl-2-butene (TME) ozonolysis: Pressure dependence of stabilized Criegee intermediates and evidence of stabilized vinyl hydroperoxides, *J. Phys. Chem. A* 115 (2011) 161-166.

[12] Y. Wu, S. Panigrahy, A.B. Sahu, et al., Understanding the antagonistic effect of methanol as a component in surrogate fuel models: A case study of methanol/n-heptane mixtures, *Combust. Flame* 226 (2021) 229-242.

[13] S.S. Nagaraja, J. Liang, S. Dong, S. Panigrahy, A. Sahu, G. Kukkadapu, S.W. Wagnon, W.J. Pitz, H.J. Curran, A hierarchical single-pulse shock tube pyrolysis study of C2–C6 1-alkenes, *Combust. Flame* 219 (2020) 456-466.

[14] S. Dong, K. Zhang, P.K. Senecal, G. Kukkadapu, S.W. Wagnon, S. Barrett, N. Lokachari, S. Panigaphy, W.J. Pitz, H.J. Curran, A comparative reactivity study of 1-alkene fuels from ethylene to 1-heptene, *Proc. Combust. Inst.* 38 (2021) 611-619.

[15] A.B. Sahu, A.A.E.-S. Mohamed, S. Panigrahy, C. Saggese, V. Patel, G. Bourque, W.J. Pitz, H.J. Curran, An experimental and kinetic modeling study of NO_x sensitization on methane autoignition and oxidation, *Combust. Flame* 238 (2022) 111746.

[16] B. Sztáray, K. Voronova, K.G. Torma, K.J. Covert, A. Bodi, P. Hemberger, T. Gerber, D.L. Osborn, CRF-PEPICO: Double velocity map imaging photoelectron photoion coincidence spectroscopy for reaction kinetics studies, *J. Chem. Phys.* 147 (2017) 013944.

[17] P. Oßwald, P. Hemberger, T. Bierkandt, E. Akyildiz, M. Köhler, A. Bodi, T. Gerber, T. Kasper, *In situ* flame

chemistry tracing by imaging photoelectron photoion coincidence spectroscopy, *Rev. Sci. Instrum.* 85 (2014) 025101.

[18] P. Hemberger, A. Bodi, T. Bierkandt, M. Köhler, D. Kaczmarek, T. Kasper, Photoelectron photoion coincidence spectroscopy provides mechanistic insights in fuel synthesis and conversion, *Energy Fuels* 35 (2021) 16265-16302.

[19] N. Hansen, T.A. Cool, P.R. Westmoreland, K. Kohse-Höinghaus, Recent contributions of flame-sampling molecular-beam mass spectrometry to a fundamental understanding of combustion chemistry, *Prog. Energy Combust. Sci.* 35 (2009) 168-191.

[20] F.N. Egolfopoulos, N. Hansen, Y. Ju, K. Kohse-Höinghaus, C.K. Law, F. Qi, Advances and challenges in laminar flame experiments and implications for combustion chemistry, *Prog. Energy Combust. Sci.* 43 (2014) 36-67.

[21] D.G. Goodwin, R.L. Speth, H.K. Moffat, B.W. Weber, Cantera: An object-oriented software toolkit for chemical kinetics, thermodynamics, and transport processes, http://www.cantera.org, Version 2.5.1, 2021.

[22] Chemical Workbench, http://www.kintechlab.com/, Version 4.1.19528, 2017.

[23] M. Schenk, L. Leon, K. Moshammer, P. Oßwald, T. Zeuch, L. Seidel, F. Mauss, K. Kohse-Höinghaus, Detailed mass spectrometric and modeling study of isomeric butene flames, *Combust. Flame* 160 (2013) 487-503.

[24] M. Gonchikzhapov, T. Kasper, Decomposition reactions of $Fe(CO)_5$, $Fe(C_5H_5)_2$, and TTIP as precursors for the spray-flame synthesis of nanoparticles in partial spray evaporation at low temperatures, *Ind. Eng. Chem. Res.* 59 (2020) 8551-8561.

[25] J. Power, K.P. Somers, S.S. Nagaraja, W. Wyrebak, H.J. Curran, Theoretical study of the reaction of hydrogen atoms with three pentene isomers: 2-Methyl-1-butene, 2-methyl-2-butene, and 3-methyl-1-butene, *J. Phys. Chem. A* 124 (2020) 10649-10666.

[26] J. Power, K.P. Somers, S.S. Nagaraja, H.J. Curran, Hierarchical study of the reactions of hydrogen atoms with alkenes: A theoretical study of the reactions of hydrogen atoms with C_2–C_4 alkenes, *J. Phys. Chem. A* 125 (2021) 5124-5145.

[27] D.M. Mintz, A. Kuppermann, Photoelectron spectroscopy of ethylene, isobutylene, trimethylethylene, and tetramethylethylene at variable angle, *J. Chem. Phys.* 71 (1979) 3499-3513.

[28] J. Pieper, S. Schmitt, C. Hemken, et al., Isomer identification in flames with double-imaging photoelectron/photoion coincidence spectroscopy (i^2PEPICO) using measured and calculated reference photoelectron spectra, *Z. Phys. Chem.* 232 (2018) 153-187.

[29] L. Ruwe, K. Moshammer, N. Hansen, K. Kohse-Höinghaus, Consumption and hydrocarbon growth processes in a 2-methyl-2-butene flame, *Combust. Flame* 175 (2017) 34-46.

[30] K. Watanabe, T. Nakayama, J. Mottl, Ionization potentials of some molecules, *J. Quant. Spectrosc. Radiat. Transf.* 2 (1962) 369-382.

[31] Z. Wang, O. Herbinet, Z. Cheng, B. Husson, R. Fournet, F. Qi, F. Battin-Leclerc, Experimental investigation of the low temperature oxidation of the five isomers of hexane, *J. Phys. Chem. A* 118 (2014) 5573-5594.

[32] P.J. Linstrom, W.G. Mallard, in, National Institute of Standards and Technology, Gaithersburg MD, 20899, https://doi.org/10.18434/T4D303, (retrieved December 3, 2021).

[33] L.A. Curtiss, P.C. Redfern, K. Raghavachari, Gaussian-4 theory, *J. Chem. Phys.* 126 (2007) 084108.

[34] M.J. Frisch, G.W. Trucks, H.B. Schlegel, et al., Gaussian 16, Revision A.03, Gaussian, Inc., Wallingford, CT, 2016.

[35] F. Turecek, L. Brabec, J. Korvola, Unstable enols in the gas phase. Preparation ionization, energies, and heats of formation of (E)- and (Z)-2-buten-2-ol, 2-methyl-1-propen-1-ol, and 3-methyl-2-buten-2-ol, *J. Am. Chem. Soc.* 110 (1988) 7984-7990.

[36] T. Bierkandt, P. Oßwald, N. Gaiser, et al., Observation of low-temperature chemistry products in laminar premixed low-pressure flames by molecular-beam mass spectrometry, *Int. J. Chem. Kinet.* 53 (2021) 1063-1081.

[37] X. Zhang, Y. Zhang, T. Li, et al., Low-temperature chemistry triggered by probe cooling in a low-pressure premixed flame, *Combust. Flame* 204 (2019) 260-267.

[38] N. Hansen, R.S. Tranter, J.B. Randazzo, J.P.A. Lockhart, A.L. Kastengren, Investigation of sampling-probe distorted temperature fields with X-ray fluorescence spectroscopy, *Proc. Combust. Inst.* 37 (2019) 1401-1408.

[39] Y. Karakaya, J. Sellmann, I. Wlokas, T. Kasper, Influence of the sampling probe on flame temperature, species, residence times and on the interpretation of ion signals of methane/oxygen flames in molecular beam mass spectrometry measurements, *Combust. Flame* 229 (2021) 111388.

[40] K. Moshammer, A.W. Jasper, D.M. Popolan-Vaida, et al., Detection and identification of the keto-hydroperoxide ($HOOCH_2OCHO$) and other intermediates during low-temperature oxidation of dimethyl ether, *J. Phys. Chem. A* 119 (2015) 7361-7374.

[41] J.P. Kercher, E.A. Fogleman, H. Koizumi, B. Sztáray, T. Baer, Heats of formation of the propionyl ion and radical and 2,3-pentanedione by threshold photoelectron photoion coincidence spectroscopy, *J. Phys. Chem. A* 109 (2005) 939-946.

[42] B. Yang, J. Wang, T.A. Cool, N. Hansen, S. Skeen, D.L. Osborn, Absolute photoionization cross-sections of some combustion intermediates, *Int. J. Mass Spectrom.* 309 (2012) 118-128.

[43] A. Fish, J.P. Wilson, The nonisothermal oxidation of 2,3-dimethylbutane, *Symp. (Int.) Combust.* 13 (1971) 229-238.

[44] X. Liu, W. Zhang, Z. Wang, et al., Dissociative photoionization of isoprene: Experiments and calculations, *J. Mass Spectrom.* 44 (2009) 404-409.

[45] G. Bieri, F. Burger, E. Heilbronner, J.P. Maier, Valence ionization energies of hydrocarbons, *Helv. Chim. Acta* 60 (1977) 2213-2233.